TOXICOLOGICAL SCIENCES **129(2)**, 411–420 (2012)
doi:10.1093/toxsci/kfs218
Advance Access publication July 21, 2012

Characterization of Mitophagy in the 6-Hydoxydopamine Parkinson's Disease Model

Maria E. Solesio,* Sara Saez-Atienzar,† Joaquin Jordán,†,[1] and Maria F. Galindo*

*Unidad de Neuropsicofarmacología Traslacional, Complejo Hospitalario Universitario de Albacete, Albacete, Spain; and
†Grupo de Neurofarmacología, Dpto. Ciencias Médicas, Fac. de Medicina de Albacete, Universidad Castilla-La Mancha, IDINE, Albacete, Spain

[1]To whom correspondence should be addressed. Fax: +34-967599327. E-mail: joaquin.jordan@uclm.es.

Received April 10, 2012; accepted June 27, 2012

In the present study, the activation of autophagy and its interaction with the mitochondrial fission machinery was investigated in an experimental model of Parkinson's disease. The addition of 50μM 6-hydroxydopamine (6-OHDA) to the dopaminergic cell line SH-SY5Y profoundly stimulated formation of autophagosomes within 12 h. Under these conditions, mitochondrial fission was also activated in a sustained manner, but this occurred at earlier time points (after 3 h). Upon 6-OHDA treatment, dynamin-related protein 1 (Drp1) transiently translocated to mitochondria, with increased levels of mitochondrial Drp1 being observed after 3 and 9 h. Pharmacological inhibition of Drp1, through treatment with the mitochondrial-division inhibitor-1 (mdivi-1), resulted in the abrogation of mitochondrial fission and in a decrease of the number of autophagic cells. In addition, 6-OHDA failed to induce the expression of the proapoptotic protein Bax in total cellular extracts although it did induce its migration to mitochondria. In our model, Bax migrated later than Drp1. However, Drp1 inhibition did not block Bax migration. These results show that reactive oxygen species but not quinone derivates act as mediators of autophagy at an early stage of the process. 6-OHDA induces hydrogen peroxide production, which was placed upstream of mitochondrial fission, given that mdivi-1 did not abrogate this increase. Furthermore, the 6-OHDA–induced activation of autophagy was also suppressed by addition of the free radical scavengers TEMPOL and MnTBAP. This effect could be reproduced by the addition of hydrogen peroxide, but not with aged 6-OHDA. To our knowledge, this is the first detailed study highlighting the various mediators that are implicated in mitochondrial alterations and autophagy of cells in response to 6-OHDA.

Key Words: **Parkinson's disease; mitochondrial dynamics; Drp1; Bax; mdivi-1; hydrogen peroxide.**

The regulation of dynamic mitochondrial processes such as fusion, fission, and mitophagy has been shown to be an important mechanism controlling cellular fate (Liesa *et al*., 2009). An imbalance in mitochondrial dynamics may contribute to both familial and sporadic neurodegenerative diseases including Parkinson's disease (PD), a progressive neurodegenerative condition that is characterized by the presence of motor and nonmotor symptoms (Cho *et al*., 2010; Lees *et al*., 2009; Su *et al*., 2010; Thomas and Beal, 2007). Evidence exists suggesting that an amplification of fission events can cause pathogenesis of human PD. Stress stimuli that are used to study PD, such as rotenone (De Palma *et al*., 2010), annonacin (Escobar-Khondiker *et al*., 2007), and 6-hydroxydopamine (6-OHDA) (Gomez-Lazaro *et al*., 2008a), are capable of inducing mitochondrial fission. Also, human fibroblasts from PD patients exhibit elevated levels of fragmented mitochondria (Exner *et al*., 2007).

Human cells contain a number of intracellular mechanisms that are essential for the removal of damaged or energy-deficient mitochondria. Macroautophagy, here simply referred to as autophagy, is one of the most prominent of these processes (Yorimitsu and Klionsky, 2005) and is important to maintain cellular homeostasis. Through the delivery of nonfunctional cytosolic proteins and organelles to lysosomes for degradation, autophagy yields a continuous turnover of cellular components (Cuervo, 2004). Undoubtedly, there are multiple connections between autophagic and apoptotic processes, which jointly can determine the fate of cells (Leber and Andrews, 2010).

Mitochondrial fission and autophagy are highly regulated process and are mediated by a defined set of proteins (Cerveny *et al*., 2001; Karbowski *et al*., 2004; Mozdy *et al*., 2000; Otsuga *et al*., 1998). One of these proteins, dynamin-related protein 1 (Drp1), is a member of the dynamin family of large GTPases and mediates the scission of mitochondrial membranes through GTP hydrolysis. Drp1 predominantly is a cytoplasmic protein that associates with mitochondrial fission sites upon oligomerization (Labrousse *et al*., 1999; Legesse-Miller *et al*., 2003). In addition, the proapoptotic Bax protein has been

colocalized to scission sites on mitochondria, suggesting that the mitochondrial fission machinery cooperates with the cell death machinery (Karbowski *et al*., 2002). In previous studies, we have shown that both proteins actively participate in the 6-OHDA preclinical model of PD (Gomez-Lazaro *et al*., 2008a,b).

Under physiological conditions, 6-OHDA is rapidly and nonenzymatically oxidized by molecular oxygen to form 1,4-para-quinone and its degradation products(Gee and Davison, 1989), along with production of ROS such as hydrogen peroxide (H_2O_2). Quinones react with nucleotic groups of macromolecules, leading to inactive or destroyed quinoproteins. H_2O_2 is central to mitochondrial oxidative damage and redox signaling, which acts as a direct redox signal independent of the accumulation of oxidative damage (Janssen-Heininger *et al*., 2008).

Hitherto, no direct observations have been reported on the effect of 6-OHDA–induced mitochondrial fission and autophagy. In the present study, we found that 6-OHDA dramatically induced mitochondrial fragmentation, resulting in an increase in autophagy through a mechanism that was meditated by reactive oxygen species and Drp1 but not by Bax.

MATERIAL AND METHODS

Reagents and plasmids. Dulbecco's modified Eagle medium (DMEM)-F12, penicillin-streptomycin, gentamicin, and fetal bovine serum (FBS) were purchased from Gibco Invitrogen, and 6-hydroxydopmaine (6-OHDA) was purchased from Sigma-Aldrich. MnTBAP and TEMPOL (4-hydroxy-2,2,6,6-tetramethylpiperidine-N-oxyl) were purchased from Calbiochem. The BCA protein assay was from Pierce, and the pDsRed2-mito vector was provided by Clontech. GFP-Bax was a gift from Dr J.H.M. Prehn (Department of Physiology and RCSI Neuroscience Research Centre, Royal College of Surgeons, Ireland), and Drp1-GFP was kindly provided by T. Wilson and Dr S. Strack (Department of Pharmacology, University of Iowa Carver College of Medicine).

Cell culture and drug treatment procedures. SH-SY5Y cell lines were obtained from the American Type Culture Collection. Cell cultures were grown in a humidified cell incubator at 37°C under a 5% CO_2 atmosphere in DMEM-F12 supplemented with 2mM L-glutamine, 20 units·ml^{-1} penicillin-streptomycin, 5 mg·ml^{-1} gentamicin, and 15% (v/v) FBS, as described previously (Jordan *et al*., 2004). 6-OHDA was added to culture medium at final concentrations of 50μM. Duration of pretreatment with the antioxidant drugs TEMPOL (0.2μM) and MnTBAP (10nM) was 30 min. For both compounds, we have verified that the treatment was not inducing cell death in control cells.

Transfections. Twenty-four hours before transfection, cells were plated at a density of 5.3 × 104 cells/cm^2 on IDIBI-coated glass dishes. Transfection was achieved using Lipofectamine reagent (Invitrogen, Carlsbad, CA) according to the manufacturer's protocol. Cells were transfected with plasmids encoding pDsRed2, Drp1-GFP, and Bax-GFP (see Solesio *et al*., forthcoming). After 4 h of incubation, the transfection mixture was removed and replaced with fresh complete medium. Experiments were performed 24 h after transfection to allow protein expression.

Analysis of mitochondrial morphology. Cells were transfected with pDsRed2-Mito, which leads to the expression of fluorescent DsRed2 in mitochondria, thereby labeling the organelles. The transfected cells were subjected to experimental treatments, and mitochondrial morphology was evaluated by fluorescence microscopy. For quantification, the percentage of cells with abnormal mitochondrial morphologies was determined and taken as a measure of the proportion of cells with fragmented mitochondria. Most of the cells had either fragmented or filamentous mitochondria, whereas a small percentage (< 10%) of the cells contained both fragmented and filamentous mitochondria. In case of the latter, the mitochondrial morphology was classified according to the majority (> 70%) of the mitochondria.

Reactive oxygen species measurement. Reactive oxygen species (ROS) in SH-SY5Ycells were detected using 2′,7′-dichlorofluorescin diacetate (H_2-DCF-DA; Molecular Probes, Eugene, OR). H_2-DCF-DA is a nonpolar compound that rapidly diffuses into cells, where it is hydrolyzed to the fluorescent polar derivative DCF and gets trapped within the cells. H_2-DCF-DA (10μM) was added to the cells. After incubation for 30 min at 37°C, the liquid was removed and KREBS was added. Intracellular ROS accumulation in cells with or without 6-OHDA treatment was measured in a Spectra Max Gemini XS (Molecular Devices). The relative level of ROS production was determined by calculating the average value from four wells in at least three independent cultures.

Image acquisition and processing. Micrographs were processed with Huygens Deconvolution Software (Scientific Volume Imaging) and Adobe Photoshop. For quantitative analysis of mitochondrial morphology, the three patterns of mitochondrial morphology (filamentous, punctuate, or intermediate) were recorded in at least 100 cells per coverslip observed on adjacent fields at magnification 63×. We assessed the robustness of this classification by comparing data obtained with separate cover slips from the same experiment and from successive passages. In addition, monitoring of the mitochondrial morphology was performed by two independent examiners on three different cultures. The proportions observed were similar in all these experiments, demonstrating that mitochondrial morphology could be reliably analyzed and did not vary within and between experiments under basal culture conditions. We performed the experiments using a "blind" counter.

Determination of subcellular concentrations of Drp1 and Bax. For measurements of subcellular concentrations of Drp1 and Bax, cells were washed with PBS and lysed for 5 min in 30 μl office-cold lysis buffer, consisting of 80mM KCl, 250mM sucrose, 500 μg/ml digitonin, and 1 μg/ml each of the protease inhibitors leupeptin, aprotinin, and pepstatin, and 0.1mM PMSF in PBS. Cell lysates were centrifuged for 5 min at 10,000 g. Protein concentrations were quantified spectrophotometrically (Micro BCA Protein Reagent Kit; Pierce, Rockford, IL), and equal amounts of protein (30 μg) were loaded onto 10% sodium dodecyl sulfate–polyacrylamide gel electrophoresis (SDS-PAGE) gels. After electrophoresis, proteins were transferred to polyvinylidene difluoride membranes (Immobilon; Millipore Corporation, Billerica, MA). Nonspecific protein binding was blocked with Blotto (4% wt/vol nonfat dried milk, 4% bovine serum albumin [Sigma], and 0.1% Tween 20 [Sigma]) in PBS for 1 h. The membranes were incubated with anti-Bax (1:1000 dilution of an anti-rabbit polyclonal, Cell Signaling) and anti-Drp1 (1:1000 dilution of anti-mouse monoclonal from BD Biosciences) overnight at 4°C. After washing with Blotto, the membranes were incubated with a secondary antibody (1:5000 dilution of a peroxidase-conjugated anti-mouse polyclonal from Promega, Madison, WI) in Blotto. The signal was detected using an enhanced chemiluminescence detection kit (GE Healthcare, Little Chalfont, Buckinghamshire, UK).

Statistics. Statistically significant differences between groups were determined by ANOVA followed by a Newman-Keuls *post hoc* analysis. The cutoff level of statistical significance was set at $p < 0.05$.

RESULTS

Autophagy is Activated by 6-OHDA Treatment

The protein LC3 has been used as a specific marker for quantification of autophagosomes, and overexpression of GFP-LC3 is a well-accepted, straightforward, and specific assessment

of autophagosome formation. Upon induction of autophagy, LC3 is conjugated to phosphatidylethanolamine and targeted to autophagic membranes. We transfected SH-SY5Y cells with GFP-LC3 and allowed its expression for 24 h prior to further treatments. When these cells were cultured in regular DMEM supplemented with 10% FBS, only a small number of GFP-LC3 dots were observed (4 ± 0.23 cell^{-1}) (Figs. 1A and B). Next, 25, 50, and 100μM 6-OHDA was added to SH-SY5Y cell cultures, and autophagosome formation was quantified at different time points. Cells with more than five autophagosomes were counted as autophagic cells. 6-OHDA induced and increased the number of GFP-LC3 dots per cell in a concentration- and time-dependent manner (Fig. 1A).

The unconjugated (LC3-I) and conjugated forms (LC3-II) of LC3 can be separated by SDS-PAGE. Immunoblot analysis showed that mock-treated SH-SY5Y cells barely contained detectable levels of LC3b-II during the 12 h of the experiment. In contrast, treatment with 50μM 6-OHDA–induced accumulation of LC3b-II, which was detectable after 12 h of treatment (Fig. 1D). The increase of LC3-II immunoreactivity correlated with a decrease of LC3-I, suggesting that autophagy occurred at a very high rate (Fig. 1D). Withdrawal of serum from the medium was used as a positive control of this event (Fig. 1D).

Drp1 Mediates 6-OHDA–Induced Mitochondrial Fission

At this point, the question arose whether autophagy is activated by mitochondrial fission. Our previous work has shown that 6-OHDA induces mitochondrial fission in SH-SY5Y cell cultures (Gomez-Lazaro *et al*., 2008a). In our current study, we have used a new approach, exploiting the pDsRed2-mito plasmid to express the mitochondrial protein DsRed2. As expected, untreated cells present mitochondria with a longitudinal aspect. Addition of 50μM 6-OHDA results in morphologically altered mitochondria, with apparently shorter filaments (Supplementary fig. 1, also see Gomez-Lazaro *et al*., 2008b). Quantitative analysis revealed that addition of 6-OHDA resulted in an increase in the proportion of cells with mitochondrial morphology

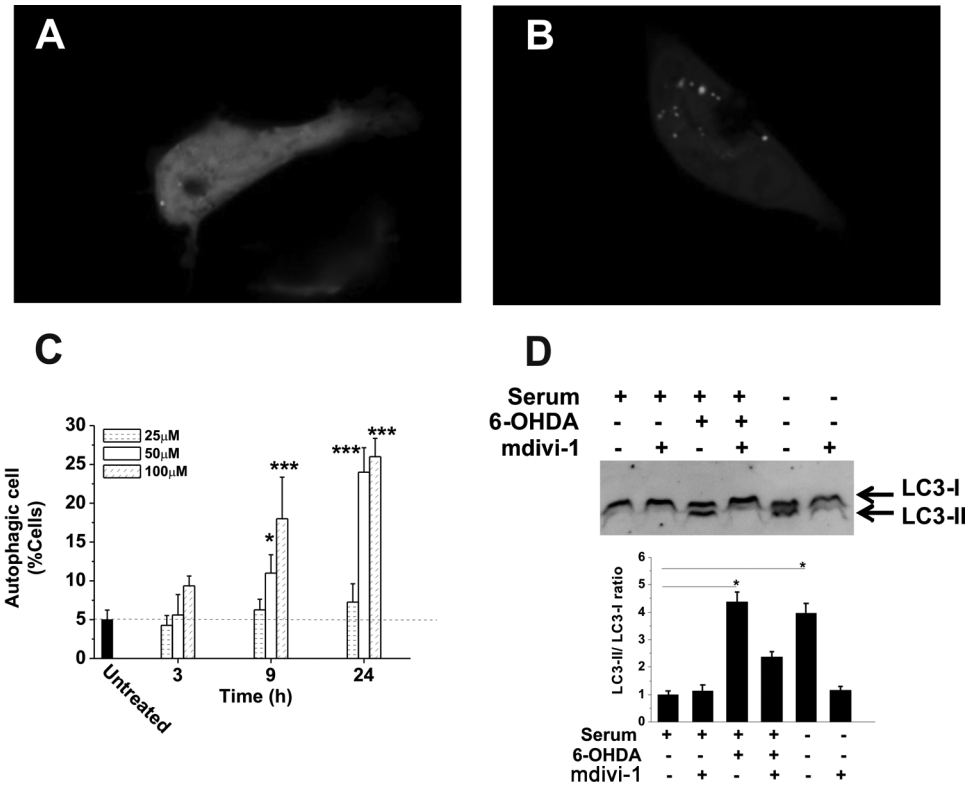

FIG. 1. 6-OHDA induces autophagy in SH-SY5Y cells. (A) Proportions of autophagic SH-SY5Y cells in cell cultures that were challenged with 0 (untreated), 25, 50, and 100μM 6-OHDA for different periods of time. Data represent mean ± SEM of four independent experiments. Significant differences between 6-OHDA–treated and untreated cells are indicated (*$p < 0.05$; ***$p < 0.001$; *t*-test). (B and C) Induction of autophagosome formation by 6-OHDA. Representative confocal fluorescent microscopy images of SH-SY5Y cells transfected with GFP-LC3 cDNA and challenged (C) or not (B) with 50μM 6-OHDA for 12 h. The punctuated distribution of green fluorescence indicates the formation of autophagosomes. (D) LC3b-II is induced by 6-OHDA. SH-SY5Y cell cultures were pretreated (or not) with 10μM mdivi-1 for 30 min before adding 50μM 6-OHDA. Serum withdrawal was used as positive control for accumulation of LC3b-II levels. Twelve hours after 50μM 6-OHDA addition, total cellular extracts were collected. Equal amounts of protein (30 μg/lane) were loaded on the gels. The immunoblot shown is representative of three independent experiments. Histograms: Quantitative analysis of the ratio of LC3-II to LC3-I ($n = 3$) (*$p < 0.05$; *t*-test).

alterations, being 24% ($p < 0.05$) after 3 h and 46% ($p < 0.01$) after 12 h of treatment. The increase in the number of cells with mitochondrial morphology alterations was already noticeable at early time points.

Drp1 is a cytosolic protein that migrates to mitochondria to induce mitochondrial fission (Lee *et al*., 2004). To gain insight in the relevance of mitochondrial fission for 6-OHDA–induced autophagy, the participation of this protein in autophagy was assayed. First, using immunoblot analysis, we demonstrated that the cellular levels of total Drp1 remained unchanged after 6-OHDA treatments, at all of the time points that were assayed (3–24 h; Fig. 2A). However, immunoblots with mitochondrial fractions revealed recruitment of Drp1 to mitochondria in SH-SY5Y cell cultures that were challenged with 6-OHDA (Fig. 2B). This effect was evident after 3 h of treatment, sustained at 9 h, and levels of mitochondrial Drp1 returned to basal levels after 24 h of treatment (Fig. 2B).

Second, SH-SY5Y cells were transfected with the fluorescent chimeric protein GFP-Drp1, which enables us to identify the intracellular localization of Drp1 using confocal microscopy. Untreated cells showed cytosolic localization of GFP-Drp1 (Fig. 2C). Upon treatment with 50μM 6-OHDA, a punctuated distribution of GFP-Drp1 was observed, indicating that Drp1 was efficiently translocated to the mitochondria in a time-dependent manner (Figs. 2D and E). The proportion of cells with a punctuated appearance of Drp1 rose to about 40% after 3 h of 6-OHDA treatment.

Next, in a pharmacological approach to investigate the relevance of this protein for autophagy, we used the Drp1-inhibitor drug mitochondria-division inhibitor-1 (mdivi-1). Incubation with mdivi-1 (10μM) led to increased length and interconnectivity of the mitochondrial network in SH-SY5Y cell cultures (Fig. 3B) and prevented 6-OHDA–induced mitochondrial fission (Fig. 3E). Subsequently, we determined the number of autophagic cells in cultures that were pretreated for 30 min with 10μM mdivi-1 before being challenged with 50μM 6-OHDA. After 12 h of 6-OHDA treatment, we determined the percentage of autophagic cells. Exposure to mdivi-1 decreased the number of autophagic cells by about 73.5% (Fig. 3F). In addition, mdivi-1 pretreatment significantly inhibited the 6-OHDA–induced accumulation of LC3b-II levels in SH-SY5Y cells after 12 h of treatment (Fig. 1D).

Bax Does Not Participate in 6-OHDA–Induced Autophagy

Previously, we have shown that Bax is a proapoptotic protein that is involved in the 6-OHDA–induced PD model (Gomez-Lazaro *et al*., 2008b). Now, we investigated the significance of Bax in 6-OHDA–induced autophagy. 6-OHDA did not induce an increase of Bax protein levels in total cellular extracts. However, we observed mitochondrial Bax recruitment 9 h after addition of 50μM 6-OHDA (Fig. 4; see Gomez-Lazaro *et al*., 2008b). Furthermore, using the fluorescent protein Bax-GFP, we observed that upon 6-OHDA treatment its appearance changed from diffuse fluorescence in the cytoplasm to a more punctuated distribution (Fig. 4A; see Gomez-Lazaro *et al*., 2008b). These results place Bax translocation downstream of mitochondrial fission in the 6-OHDA–induced PD model.

Subsequently, we analyzed whether Drp1 inhibition would modulate 6-OHDA–induced Bax translocation. Cell cultures were pretreated with mdivi-1 for 30 min prior to the addition of 50μM 6-OHDA. Twelve hours after 6-OHDA addition, mdivi-1 pretreated cell cultures presented a comparable number of cells with a punctuated GFP-Bax distribution as mdivi-1-untreated control cells (Fig. 4D).

Next, we studied the significance of Bax in 6-OHDA–induced autophagy. Mouse embryonic fibroblasts (MEFs) from wild-type and Bax knockout animals ($Bax^{-/-}$MEFs) were transfected with GFP-LC3 plasmid, 24 h before exposure to 50μM 6-OHDA. As shown in Figure 4E, the lack of Bax did not decrease the percentage of autophagic cells in Bax knockout animals 12 h after 6-OHDA addition compared with wild-type MEF cells.

ROS Participate in 6-OHDA–Induced Autophagy

Under physiological conditions, 6-OHDA is rapidly and nonenzymatically oxidized to form 1,4-para-quinone and its degradation products (Gee and Davison, 1989), along with production of ROS such as H_2O_2. To determine whether ROS participate in our model, we used the dye CM-H_2DCF-DA to measure peroxide-like formation. Differences in cellular H_2O_2 during different treatments were examined by comparing the 2′,7′-dichlorofluorescein (DCF) formation in cells challenged or not with 6-OHDA (Fig. 5A). There was significant increase in DCF fluorescence levels by 3 h after treatment. Furthermore, the pretreatment with mitochondrial fission inhibitor mdivi-1 did not decrease this rise in ROS production. (Fig. 5A).

The role of ROS in our model was approached using two broad spectrum antioxidant drugs, TEMPOL and MnTBAP. Both ROS-scavenger drugs abrogated the increase in the number of 6-OHDA–induced autophagic cells, 12 h after 6-OHDA treatments (Fig. 5B). Furthermore, we challenged the cell cultures with 100μM H_2O_2. After 12 h of treatment, H_2O_2 induced a robust increase in autophagy (Fig. 5B).

We used aged 6-OHDA, which has lost the ROS-inductor capacity, to investigate the role of quinone derivates. Cell cultures were treated with 50μM aged 6-OHDA, and autophagy activation was assayed. As shown in histograms, aged 6-OHDA failed to induce an increase in the number autophagosomes per cell (Fig. 5B).

DISCUSSION

A number of studies have investigated mitochondrial dynamics in different PD models. However, none of these have directly compared the activation of mitochondrial fission and autophagy in the human neuroblastoma cell model of PD as a consequence 6-OHDA addition. We took advantage of

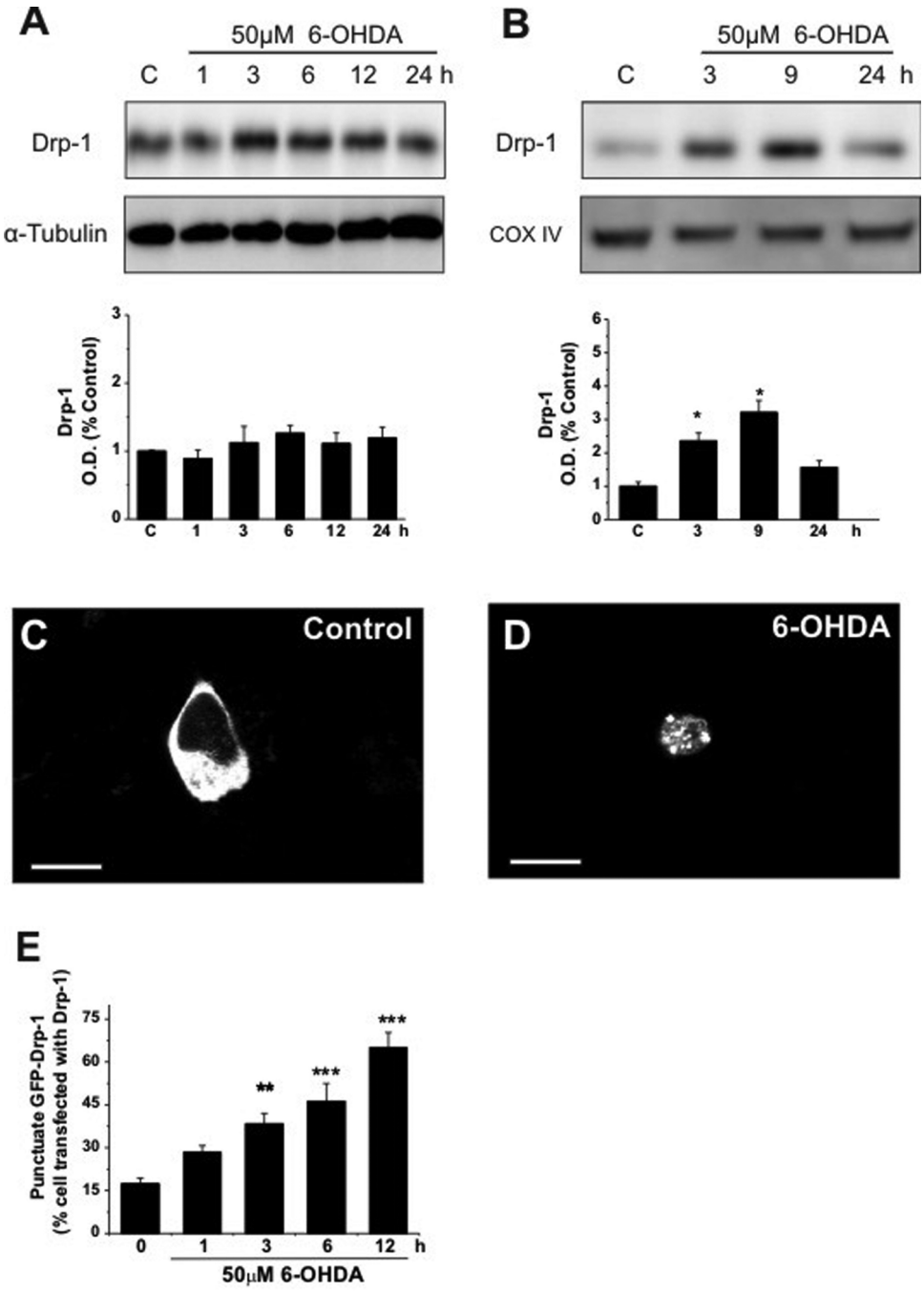

FIG. 2. Drp1 participates in 6-OHDA–induced mitochondrial fragmentation. (A and B) Immunoblot analysis showing Drp1 levels in total cellular extracts (A) and mitochondrial fractions (B) of SH-SY5Y cells that were challenged with 50μM 6-OHDA for the indicated periods of time. Equal amounts of protein (30 μg/lane) were loaded on the gels. α-Tubulin levels were used as an index of total cell load, COX-IV was used as an index of mitochondrial load. The immunoblots shown are representative of three independent experiments. Histograms: Variation of Drp1 levels normalized to α-Tubulin or COX is shown. Results are expressed as mean ± SEM ($n = 3$). (C and D) Confocal imaging of SH-SY5Y cells that were transfected with Drp1-GFP and treated (D) or not (C) with 50μM 6-OHDA for 3 h. Images shown are representative of four independent experiments. In each case, several cells were examined. Scale bars: 10 μm. (E) Percentages of cells with punctuate Drp1 distribution. Results shown are the mean ± SEM of at least three experiments, each performed in triplicate. Significant differences between 6-OHDA–treated cells and controls are indicated (**$p < 0.01$).

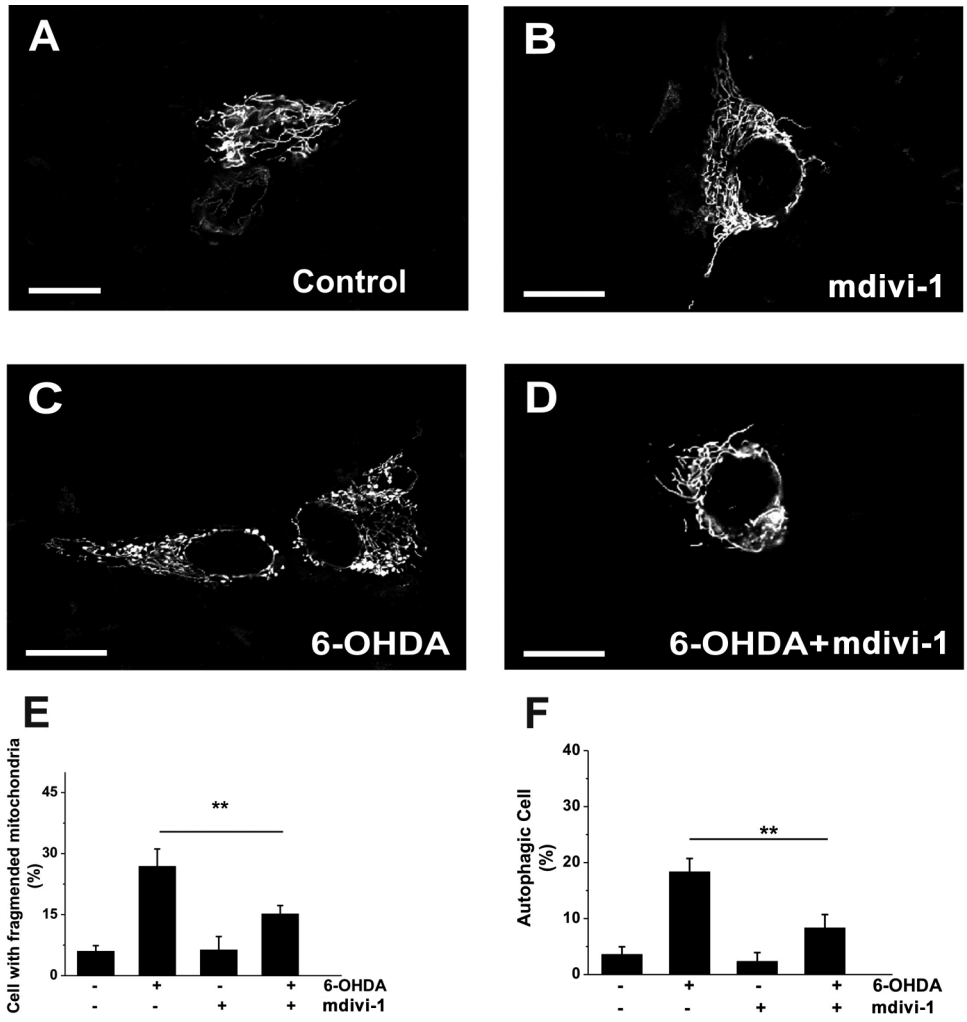

FIG. 3. Drp1 inhibition blocks 6-OHDA–induced mitochondrial morphology alteration and autophagy. (A–D) Representative confocal images of SH-SY5Y cells that were transfected with the pDsRed2-mito vector. Cells were pretreated (B and D) or not (A and C) with 10μM mdivi-1 prior to a 3 h treatment with 50μM 6-OHDA (C and D). Scale bars: 10 μm. (E) Proportions of cells with fragmented mitochondrial patterns were determined after a 3 h treatment with 6-OHDA. (F) Proportions of autophagic cells in parallel cell cultures after 12 h of 6-OHDA treatment. Data in histograms are the mean ± SEM of four independent experiments (**$p < 0.01$; one way ANOVA *post hoc* Tukey).

GFP-fusions to Drp1, Bax, and LC3 to study mitochondrial morphology alterations, Bax translocation, and autophagy in time-course experiments, and we used a pharmacological approach to elucidate plausible interrelationships between these events.

Consistent with our previous observations (Gomez-Lazaro *et al*., 2008a), SH-SY5Y cell cultures showed a significant increase in the percentage of cells with truncated or fragmented mitochondria upon 6-OHDA treatment. This process was dependent on the mitochondrial fission factor Drp1. Drp1 is a cytosolic protein that forms oligomers, which are recruited to the outer mitochondrial membrane and constrict the organelle in a GTPase-dependent manner (Fukushima *et al*., 2001; Zhu *et al*., 2004). We observed that Drp1 translocated to mitochondria 3 h after addition of 50μM 6-OHDA although the levels of total Drp1 were unchanged in cellular extracts. The relevance of this protein for mitochondrial fission was evidenced further by pretreating the cells with the mdivi-1. mdivi-1 prevents docking of Drp1 at the mitochondrial outer membrane and, consequently, reduces mitochondrial fission after several insults (Cassidy-Stone *et al*., 2008; Cereghetti *et al*., 2008). Consistent with this, we observed that mdivi-1 significantly attenuated 6-OHDA–induced mitochondrial fission.

After 6-OHDA addition, the proapoptotic protein Bax also translocated from the cytosol to the mitochondria in SH-SY5Y cells. In our experimental model, this process took place after mitochondrial fragmentation and Drp1 translocation. SH-SY5Y cells consistently showed mitochondrial Bax localization 6 h after 6-OHDA addition. We were unable to find mitochondrial Bax-aggregation loci at the very early time points where

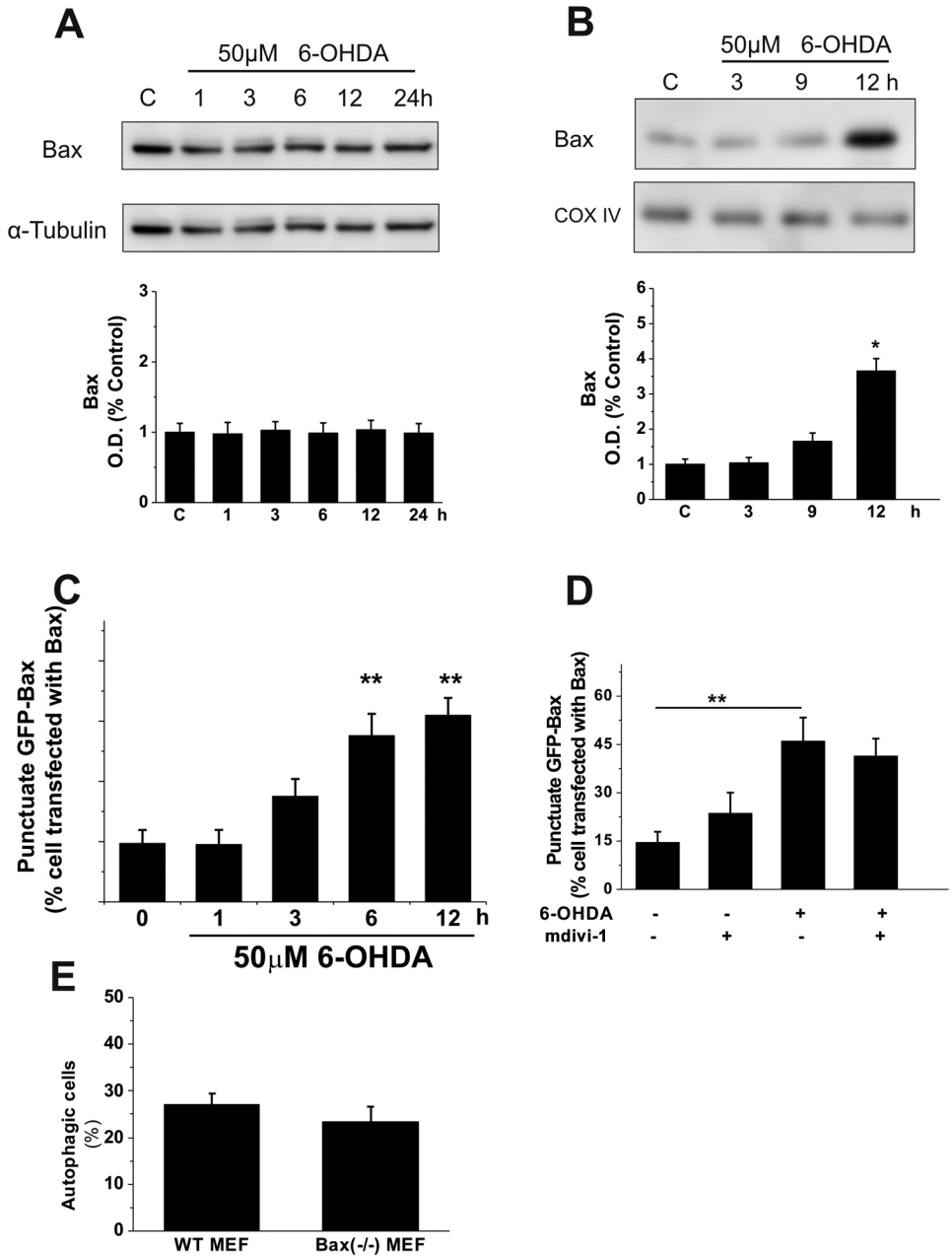

FIG. 4. 6-OHDA induces autophagy in a Bax-independent manner. (A and B) Immunoblot analysis of Bax protein levels in total cellular extracts (A) and mitochondrial fractions (B) of SH-SY5Y cells that were challenged with 50μM 6-OHDA for the periods of time indicated. Equal amounts of protein (30 μg per lane) were loaded on the gels. The immunoblots shown are representative of three independent experiments. Histograms: Variation of Bax levels normalized to COX or α-Tubulin is shown. Results are expressed as mean ± SEM ($n = 3$). (C) Percentages of cells with punctuate Bax distribution upon a 12 h treatment with 50μM 6-OHDA. (D) Drp1 inhibition failed to block Bax translocation. Cell cultures overexpressing Bax-GFP were pretreated (or not) with mdivi-1 for 30 min prior to the addition of 50μM 6-OHDA. After 12 h of 6-OHDA treatment, the percentages of cells with punctuate Bax-GFP distribution were determined. (E) Lack of Bax protein expression does not affect the autophagosome formation that is triggered by 6-OHDA. Percentages of autophagic cells, determined as the proportions of MEF cells expressing LC3-GFP, upon a 12 h treatment with 50μM 6-OHDA. Cells with more than 5 LC3-GFP dots were considered positive. In C–E, data are the mean ± SEM of at least three independent experiments, each performed in triplicate. Significant differences between treated cells and controls are indicated (**$p < 0.01$).

mitochondrial fragmentation was already evident (< 3 h of treatment). mdivi-1 failed to abrogate the translocation of Bax to the mitochondria upon 6-OHDA additions. Consequently, the 6-OHDA–induced mitochondrial Bax translocation was independent of Drp1 and mitochondrial fission. In agreement with this, in Drp1$^{-/-}$ cells (Ishihara *et al.*, 2009) or in cells that were transfected with a dominant negative allele, DrpK38A, that is defective in GTP binding (Frank *et al.*, 2001; Germain

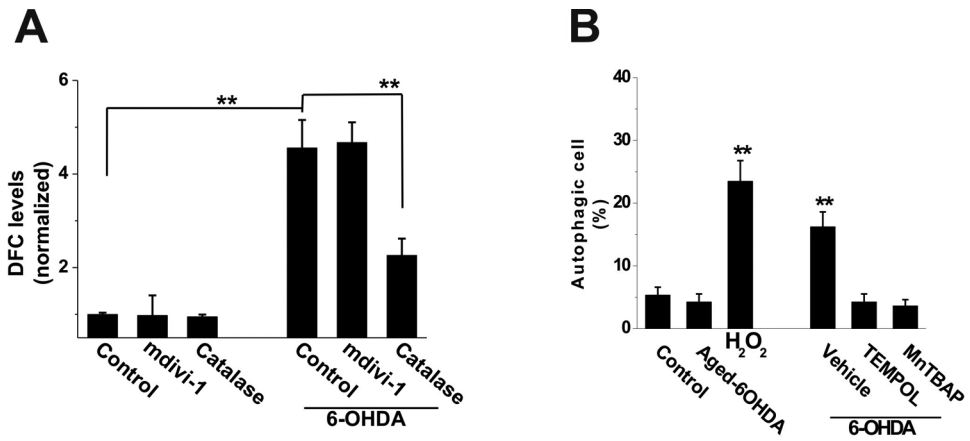

FIG. 5. ROS function as second messengers in 6-OHDA–induced mitochondrial fragmentation and autophagy. (A) Effect of 6-OHDA on the MitoP/MitoB ratio in SH-SY5Y cells. Cells that had been incubated with MitoB were incubated under 50μM 6-OHDA for 3 h, and then the MitoP/MitoB ratio was determined. Data are means ± SEM of three replicates. (B) Proportions of autophagic cells were determined in at least six different cultures under basal conditions (control) and after 12 h of treatments. Cell cultures overexpressing GFP-LC3 protein were challenged either with 50μM aged 6-OHDA or with 100μM H_2O_2. Parallel cultures were preincubated with 0.2μM TEMPOL or 10nM MnTBAP for 30 min prior to treatment with 6-OHDA. Given values are the mean ± SEM of five independent experiments that were performed in quadruplicate. (*$p < 0.05$; **$p < 0.001$; one-way ANOVA *post hoc* Tukey; $p > 0.05$).

et al., 2005; Karbowski *et al*., 2002; Lee *et al*., 2004), Bax translocates to the mitochondria with kinetics similar to those observed in wild-type cells. Moreover, mitochondrial release of proapoptotic proteins, as Smac/DIABLO, is not affected by the absence of Drp1 (Estaquier and Arnoult, 2007; Parone *et al*., 2006). Accordingly, Bax is dispensable for mitochondrial fission in the 6-OHDA model (Gomez-Lazaro *et al*., 2008a) but also when fission is induced by hFis1 or by a widely used intrinsic apoptotic stimulus (Gomez-Lazaro *et al*., 2008a).

Our results showed that autophagy is induced by 6-OHDA treatment. The 6-OHDA–induced autophagy correlated with an increase in the LC3-II protein level and with the accumulation of autophagic vacuoles in the cytoplasm. Consistent with our data, accumulation of autophagic vacuoles and activation of lysosomes have been observed in nigral rat neurons that had been treated with 6-OHDA (Li *et al*., 2011). Autophagy seems to be involved in mitochondrial quality control by promoting the removal of damaged mitochondria. Our data indicate the involvement of autophagy in the degradation of altered mitochondria. To establish this further, we monitored autophagosome formation in cells that were coexpressing GFP-LC3 and the mitochondrial protein DsRed2. Among the total mitochondrial population, autophagosomes appeared to associate specifically with fragmented mitochondria. In 6-OHDA–challenged SH-SY5Y cells, the formation of autophagosomes took place distant from the mitochondria and in a time-dependent manner. The autophagosomes specifically approach fragmented mitochondria, as indicated by the observed colocalization at the later time points of 6-OHDA treatment. Consistent with our data, the mitochondrial quality control hypothesis postulates that dysfunctional mitochondria are susceptible to degradation (Twig *et al*., 2008) and that mitochondrial elongation serves to protect mitochondria from mitophagy (Gomes *et al*., 2011; Rambold *et al*., 2011). Another study has shown that cytoplasmic components are degraded during the initial period of starvation (0–6 h), whereas mitochondria become a substrate of lysosomes much later (Kristensen *et al*., 2008). It remains to be determined whether the induction of autophagy by 6-OHDA is related to cell death or to a cytoprotective response, which is activated by dying cells in order to cope with stress. In a previous study, tyrosine hydrolase–positive neurons in substantia nigra were protected from 6-OHDA–induced cell death when they were pretreated with the autophagy inhibitor 3-methyladenine (Li *et al*., 2011). On the other hand, experiments using neuron-specific knockout mouse models have demonstrated that autophagy deficiency leads to protein aggregation and neurodegeneration, even in the absence of disease-related aggregate-prone proteins (He and Klionsky, 2006).

Further, we investigated the signaling pathways that are involved in 6-OHDA–induced mitochondrial fission and autophagy, which revealed a key role for ROS. Our data demonstrated a relationship between ROS and 6-OHDA–induced mitochondrial fission and, subsequently, mitophagy. Intriguingly, 6-OHDA increases H_2O_2 between the cells. We reach this observation using the dye CM-H2DCF-DA to measure peroxide-like formation. This specific toll allows us ascertain the role of ROS into the mitochondrial dynamic process. Thus, H_2O_2 production is upstream of mitochondrial fission, given that the inhibition of this dynamic process, by mdivi-1, did not block mitochondrial H_2O_2 after 6-OHDA treatments. In addition, TEMPOL and MnTBAP, two well-known antioxidant drugs, abolished translocation of Drp1 to mitochondria and, consequently, 6-OHDA–induced mitochondrial fission. In keeping with this interpretation, oxidative stress might be

responsible for induced mitochondrial fission in several processes, including PD, perhaps due to a redox posttranslational change in Drp1 protein (Nakamura and Lipton, 2010, 2011).

In conclusion, our findings show that 6-OHDA induces autophagy in human SH-SY5Y cells, which is mediated in part by the mitochondrial fission signaling pathways. Furthermore, ROS contribute to fission and autophagy in this neurodegenerative disease model. Deciphering the signaling cascades that underlie mitophagy triggered by 6-OHDA in SH-SY5Y cell cultures, as well as the mechanisms that determine the selectivity of this response, will help to better understand this process and may have impact on human treatment strategies of PD.

SUPPLEMENTARY DATA

Supplementary data are available online at http://toxsci.oxfordjournals.org/.

ACKNOWLEDGMENTS

We thank Carlos Garrido for technical help, and T. Wilson, Dr S. Strack and Dr J.H.M. Prehn for providing vectors.

FUNDING

This work was supported by SAF2008-05143-C03-1 from Ministerio de Ciencia e Innovación and PI2007/55 Consejería de Sanidad from Junta de Comunidades de Castilla-La Mancha (to J.J.) and by 'Incorporación de grupos emergentes' FIS CARLOS III (EMER07/023) and FIS-FEDER (PI080693; PI-2008/21 to M.F.G.). M.E.S. is a FIS-FEDER grant fellow.

REFERENCES

Cassidy-Stone, A., Chipuk, J. E., Ingerman, E., Song, C., Yoo, C., Kuwana, T., Kurth, M. J., Shaw, J. T., Hinshaw, J. E., Green, D. R., *et al.* (2008). Chemical inhibition of the mitochondrial division dynamin reveals its role in Bax/Bak-dependent mitochondrial outer membrane permeabilization. *Dev. Cell* **14,** 193–204.

Cereghetti, G. M., Stangherlin, A., Martins de Brito, O., Chang, C. R., Blackstone, C., Bernardi, P., and Scorrano, L. (2008). Dephosphorylation by calcineurin regulates translocation of Drp1 to mitochondria. *Proc. Natl. Acad. Sci. U.S.A.* **105,** 15803–15808.

Cerveny, K. L., McCaffery, J. M., and Jensen, R. E. (2001). Division of mitochondria requires a novel DMN1-interacting protein, Net2p. *Mol. Biol. Cell* **12,** 309–321.

Cho, D. H., Nakamura, T., and Lipton, S. A. (2010). Mitochondrial dynamics in cell death and neurodegeneration. *Cell. Mol. Life Sci.* **67,** 3435–3447.

Cuervo, A. M. (2004). Autophagy: Many paths to the same end. *Mol. Cell. Biochem.* **263,** 55–72.

De Palma, C., Falcone, S., Pisoni, S., Cipolat, S., Panzeri, C., Pambianco, S., Pisconti, A., Allevi, R., Bassi, M. T., Cossu, G., *et al.* (2010). Nitric oxide inhibition of Drp1-mediated mitochondrial fission is critical for myogenic differentiation. *Cell Death Differ.* **17,** 1684–1696.

Escobar-Khondiker, M., Höllerhage, M., Muriel, M. P., Champy, P., Bach, A., Depienne, C., Respondek, G., Yamada, E. S., Lannuzel, A., Yagi, T., *et al.* (2007). Annonacin, a natural mitochondrial complex I inhibitor, causes tau pathology in cultured neurons. *J. Neurosci.* **27,** 7827–7837.

Estaquier, J., and Arnoult, D. (2007). Inhibiting Drp1-mediated mitochondrial fission selectively prevents the release of cytochrome c during apoptosis. *Cell Death Differ.* **14,** 1086–1094.

Exner, N., Treske, B., Paquet, D., Holmström, K., Schiesling, C., Gispert, S., Carballo-Carbajal, I., Berg, D., Hoepken, H. H., Gasser, T., *et al.* (2007). Loss-of-function of human PINK1 results in mitochondrial pathology and can be rescued by parkin. *J. Neurosci.* **27,** 12413–12418.

Frank, S., Gaume, B., Bergmann-Leitner, E. S., Leitner, W. W., Robert, E. G., Catez, F., Smith, C. L., and Youle, R. J. (2001). The role of dynamin-related protein 1, a mediator of mitochondrial fission, in apoptosis. *Dev. Cell* **1,** 515–525.

Fukushima, N. H., Brisch, E., Keegan, B. R., Bleazard, W., and Shaw, J. M. (2001). The GTPase effector domain sequence of the Dnm1p GTPase regulates self-assembly and controls a rate-limiting step in mitochondrial fission. *Mol. Biol. Cell* **12,** 2756–2766.

Gee, P., and Davison, A. J. (1989). Intermediates in the aerobic autoxidation of 6-hydroxydopamine: Relative importance under different reaction conditions. *Free Radic. Biol. Med.* **6,** 271–284.

Germain, M., Mathai, J. P., McBride, H. M., and Shore, G. C. (2005). Endoplasmic reticulum BIK initiates DRP1-regulated remodelling of mitochondrial cristae during apoptosis. *EMBO J.* **24,** 1546–1556.

Gomes, L. C., Di Benedetto, G., and Scorrano, L. (2011). During autophagy mitochondria elongate, are spared from degradation and sustain cell viability. *Nat. Cell Biol.* **13,** 589–598.

Gomez-Lazaro, M., Bonekamp, N. A., Galindo, M. F., Jordán, J., and Schrader, M. (2008a). 6-Hydroxydopamine (6-OHDA) induces Drp1-dependent mitochondrial fragmentation in SH-SY5Y cells. *Free Radic. Biol. Med.* **44,** 1960–1969.

Gomez-Lazaro, M., Galindo, M. F., Concannon, C. G., Segura, M. F., Fernandez-Gomez, F. J., Llecha, N., Comella, J. X., Prehn, J. H., and Jordan, J. (2008b). 6-Hydroxydopamine activates the mitochondrial apoptosis pathway through p38 MAPK-mediated, p53-independent activation of Bax and PUMA. *J. Neurochem.* **104,** 1599–1612.

He, C., and Klionsky, D. J. (2006). Autophagy and neurodegeneration. *ACS Chem. Biol.* **1,** 211–213.

Ishihara, N., Nomura, M., Jofuku, A., Kato, H., Suzuki, S. O., Masuda, K., Otera, H., Nakanishi, Y., Nonaka, I., Goto, Y., *et al.* (2009). Mitochondrial fission factor Drp1 is essential for embryonic development and synapse formation in mice. *Nat. Cell Biol.* **11,** 958–966.

Janssen-Heininger, Y. M., Mossman, B. T., Heintz, N. H., Forman, H. J., Kalyanaraman, B., Finkel, T., Stamler, J. S., Rhee, S. G., and van der Vliet, A. (2008). Redox-based regulation of signal transduction: Principles, pitfalls, and promises. *Free Radic. Biol. Med.* **45,** 1–17.

Jordan, J., Galindo, M. F., Tornero, D., González-García, C., and Ceña, V. (2004). Bcl-x L blocks mitochondrial multiple conductance channel activation and inhibits 6-OHDA-induced death in SH-SY5Y cells. *J. Neurochem.* **89,** 124–133.

Karbowski, M., Jeong, S. Y., and Youle, R. J. (2004). Endophilin B1 is required for the maintenance of mitochondrial morphology. *J. Cell Biol.* **166,** 1027–1039.

Karbowski, M., Lee, Y. J., Gaume, B., Jeong, S. Y., Frank, S., Nechushtan, A., Santel, A., Fuller, M., Smith, C. L., and Youle, R. J. (2002). Spatial and temporal association of Bax with mitochondrial fission sites, Drp1, and Mfn2 during apoptosis. *J. Cell Biol.* **159,** 931–938.

Kristensen, A. R., Schandorff, S., Høyer-Hansen, M., Nielsen, M. O., Jäättelä, M., Dengjel, J., and Andersen, J. S. (2008). Ordered organelle

degradation during starvation-induced autophagy. *Mol. Cell Proteomics* **7,** 2419–2428.

Labrousse, A. M., Zappaterra, M. D., Rube, D. A., and van der Bliek, A. M. (1999). C. elegans dynamin-related protein DRP-1 controls severing of the mitochondrial outer membrane. *Mol. Cell* **4,** 815–826.

Leber, B., and Andrews, D. W. (2010). Closing in on the link between apoptosis and autophagy. *F1000 Biol. Rep.* **2,** 88.

Lee, Y. J., Jeong, S. Y., Karbowski, M., Smith, C. L., and Youle, R. J. (2004). Roles of the mammalian mitochondrial fission and fusion mediators Fis1, Drp1, and Opa1 in apoptosis. *Mol. Biol. Cell* **15,** 5001–5011.

Lees, A. J., Hardy, J., and Revesz, T. (2009). Parkinson's disease. *Lancet* **373,** 2055–2066.

Legesse-Miller, A., Massol, R. H., and Kirchhausen, T. (2003). Constriction and Dnm1p recruitment are distinct processes in mitochondrial fission. *Mol. Biol. Cell* **14,** 1953–1963.

Li, L., Wang, X., Fei, X., Xia, L., Qin, Z., and Liang, Z. (2011). Parkinson's disease involves autophagy and abnormal distribution of cathepsin L. *Neurosci. Lett.* **489,** 62–67.

Liesa, M., Palacín, M., and Zorzano, A. (2009). Mitochondrial dynamics in mammalian health and disease. *Physiol. Rev.* **89**, 799–845.

Mozdy, A. D., McCaffery, J. M., and Shaw, J. M. (2000). Dnm1p GTPase-mediated mitochondrial fission is a multi-step process requiring the novel integral membrane component Fis1p. *J. Cell Biol.* **151,** 367–380.

Nakamura, T., and Lipton, S. A. (2010). Redox regulation of mitochondrial fission, protein misfolding, synaptic damage, and neuronal cell death: Potential implications for Alzheimer's and Parkinson's diseases. *Apoptosis* **15,** 1354–1363.

Nakamura, T., and Lipton, S. A. (2011). Redox modulation by S-nitrosylation contributes to protein misfolding, mitochondrial dynamics, and neuronal synaptic damage in neurodegenerative diseases. *Cell Death Differ.* **18,** 1478–1486.

Otsuga, D., Keegan, B. R., Brisch, E., Thatcher, J. W., Hermann, G. J., Bleazard, W., and Shaw, J. M. (1998). The dynamin-related GTPase, Dnm1p, controls mitochondrial morphology in yeast. *J. Cell Biol.* **143,** 333–349.

Parone, P. A., James, D. I., Da Cruz, S., Mattenberger, Y., Donzé, O., Barja, F., and Martinou, J. C. (2006). Inhibiting the mitochondrial fission machinery does not prevent Bax/Bak-dependent apoptosis. *Mol. Cell. Biol.* **26,** 7397–7408.

Rambold, A. S., Kostelecky, B., Elia, N., and Lippincott-Schwartz, J. (2011). Tubular network formation protects mitochondria from autophagosomal degradation during nutrient starvation. *Proc. Natl. Acad. Sci. U.S.A.* **108,** 10190–10195.

Solesio, M. E., Saez-Atienzar, S., Jordan, J., and Galindo, M. F. (forthcoming). 3-Nitropropionioc acid induces autophagy by mitochondrial permeability transition pore formation rather than activation of the mitochondrial fission pathway. *Br. J. Pharmacol*.

Su, B., Wang, X., Zheng, L., Perry, G., Smith, M. A., and Zhu, X. (2010). Abnormal mitochondrial dynamics and neurodegenerative diseases. *Biochim. Biophys. Acta* **1802,** 135–142.

Thomas, B., and Beal, M. F. (2007). Parkinson's disease. *Hum. Mol. Genet.* **16,** R183–R194.

Twig, G., Elorza, A., Molina, A. J., Mohamed, H., Wikstrom, J. D., Walzer, G., Stiles, L., Haigh, S. E., Katz, S., Las, G., *et al.* (2008). Fission and selective fusion govern mitochondrial segregation and elimination by autophagy. *EMBO J.* **27,** 433–446.

Yorimitsu, T., and Klionsky, D. J. (2005). Autophagy: Molecular machinery for self-eating. *Cell Death Differ.* **12** (Suppl. 2), 1542–1552.

Zhu, P. P., Patterson, A., Stadler, J., Seeburg, D. P., Sheng, M., and Blackstone, C. (2004). Intra- and intermolecular domain interactions of the C-terminal GTPase effector domain of the multimeric dynamin-like GTPase Drp1. *J. Biol. Chem.* **279,** 35967–35974.